

Spin-polarized scanning tunneling microscopy of half-metallic ferromagnets: Non-quasiparticle contributions

V. Yu. Irkhin

Institute of Metal Physics, 620219 Ekaterinburg, Russia

M. I. Katsnelson

Institute of Molecules and Materials, University of Nijmegen, 6525 ED Nijmegen, The Netherlands

The role of the many-body (spin-polaronic) effects in the scanning tunneling spectroscopy of half-metallic ferromagnets (HMF) is considered. It is shown that the non-quasiparticle (NQP) states exist in the majority or minority spin gap in the presence of arbitrary external potential and, in particular, at the surfaces and interfaces. Energy dependence of the NQP density of states is obtained in various models of HMF, an important role of the hybridization nature of the energy gap being demonstrated. The corresponding temperature dependence of spin polarization is calculated. It is shown that the NQP states result in a sharp bias dependence of the tunneling conductance near zero bias. Asymmetry of the NQP states with respect to the Fermi energy provides an opportunity to separate phonon and magnon peaks in the inelastic spectroscopy by STM.

I. INTRODUCTION

The history of the investigations of half-metallic ferromagnets (HMF) starts from the electronic structure calculation for NiMnSb [1]; later a number of other examples were discovered, e.g., CrO₂, Fe₃O₄, a number of the Heusler alloys Co₂MnZ and RMnSb (for a review, see Refs. 2, 3). These substances have metallic electronic structure for one spin projection (majority- or minority-spin states), but for the opposite spin direction the Fermi level lies in the energy gap. Owing to this fact HMF attract now a growing attention of researchers in connection with “spintronics”, or spin-dependent electronics [4]. The spin-up and spin-down contributions to electronic transport properties have different orders of magnitude, which can result in a huge magnetoresistance for heterostructures containing HMF [2]. Some evidences of the HMF behavior in colossal magnetoresistance (CMR) materials like La_{1-x}Sr_xMnO₃ found by using tunneling spectroscopy [5, 6] and photoemission technique [7] have increased considerably the interest in the half-metallic ferromagnetism; however, the situation in the CMR systems is controversial, as demonstrate Andreev reflection experiments [8].

Peculiar band structure of HMF results in an important role of incoherent (non-quasiparticle, NQP) states which occur because of correlation effects [2]. The appearance of NQP states in the energy gap near the Fermi level [9, 10, 11, 12] is one of the most interesting correlation effects typical for HMF. The origin of these states is connected with “spin-polaron” processes: the spin-down low-energy electron excitations, which are forbidden for HMF in the one-particle picture, turn out to be possible as superpositions of spin-up electron excitations and virtual magnons. The density of these states vanishes at the Fermi level E_F for temperature $T = 0$, but increases drastically at the energy scale of the order of a characteristic magnon frequency $\bar{\omega}$. The existence of NQP states is relevant for spin-polarized electron spectroscopy [12, 13], NMR [14], core-level spectra of the HMF [15], and subgap transport in ferromagnet-superconductor junctions (Andreev reflection) [16]. Several experiments could be performed in order to clarify the impact of the NQP states on spintronics. In particular, $I - V$ characteristics of half-metallic tunnel junctions for the case of antiparallel spins are completely determined by NQP states [17, 18]. Recently the density of NQP states has been calculated from first principles for a prototype HMF, NiMnSb [19], and for CrAs [20].

On the other hand, HMF are very interesting conceptually as a class of materials which may be convenient to treat many-body solid state physics that is essentially beyond band theory. It is accepted that usually many-body effects lead only to renormalization of the quasiparticle parameters in the sense of Landau’s Fermi liquid (FL) theory, the electronic *liquid* being *qualitatively* similar to the electron *gas* (see, e.g., Refs. 21, 22). On the other hand, NQP states in HMF are not described by the FL theory. As an example of highly unusual properties of the NQP states, we note that they can contribute to the T -linear term in the electron heat capacity [12, 23], despite their density at E_F is zero for $T = 0$.

Spin-polarized scanning tunneling microscopy (STM) [24] is a very efficient new method which enables one to probe directly the spectral density with spin resolution in magnetic systems. The spin-polarized STM should be able to probe the NQP states via their contribution to the differential tunneling conductivity dI/dV . At zero temperature, NQP states arise only above E_F for the case of minority-spin gap and only below E_F for the majority-gap HMF [2]. Unlike the photoemission spectroscopy which probes only occupied electron states, STM detects the states both above and below E_F , depending on the sign of bias.

Theoretical investigation of NQP contributions to STM spectra is the aim of the present paper. The paper is

organized as follows. In Sect.2 we discuss a general expression for the tunneling current \mathcal{I} as applied to HMF. In Sect.3 the effect of surface potential and other spatial inhomogeneities on the NQP spectral density is considered. In Sects.4 and 5 we calculate the energy and temperature dependences of $d\mathcal{I}/dV$ and treat the problem of tunneling-current spin-polarization at finite temperatures. In Sect.6 the bias dependences of the tunneling conductance are discussed.

II. CALCULATION OF THE TUNNELING CURRENT

A general expression for the tunneling current in the lowest order in the tunneling matrix elements has the form [25, 26]

$$\mathcal{I} = \frac{\pi e}{\hbar} \sum_{n\nu\sigma} |M_{n\nu}^\sigma|^2 \int dE \mathcal{A}_n^\sigma(E) \mathcal{A}_\nu^\sigma(E - eV) [f(E - eV) - f(E)] \quad (1)$$

where e is electron charge, σ is the spin projection, V is the bias, $f(\varepsilon)$ is the Fermi distribution function, Greek (Latin) indices label electron eigenstates for the sample (tip) $\psi_{n\sigma}, \psi_{\nu\sigma}$

$$M_{n\nu}^\sigma = \frac{\hbar^2}{2m} \int d\mathbf{A} (\psi_{n\sigma}^* \nabla \psi_{\nu\sigma} - \psi_{\nu\sigma}^* \nabla \psi_{n\sigma}) \quad (2)$$

is the current matrix element, m is the free electron mass (the surface integral in Eq.(2) is taken over arbitrary area between the tip and the sample), and

$$\mathcal{A}_\nu^\sigma(E) = -\frac{1}{\pi} \text{Im} G_\nu^\sigma(E) \quad (3)$$

is the corresponding spectral density, $G_\nu^\sigma(E) = G_{\nu\nu}^\sigma(E)$ is the sample Green's function,

$$G_{\nu\lambda}^\sigma(E) = \langle \langle c_{\nu\sigma} | c_{\lambda\sigma}^\dagger \rangle \rangle_E,$$

$c_{\nu\sigma}^\dagger$ being the creation operators for conduction electrons. It is worthwhile to emphasize that the expression (1) takes into account correlation effects in a formally exact way, assuming that the tunneling probability is small. In fact, the latter condition should be satisfied for proper STM measurements, otherwise they cannot be considered as a true probe. In the WKB approximation Eq.(1) takes the form [27]

$$\mathcal{I}(z, V) \simeq \frac{\pi e}{\hbar} \left(\frac{\hbar^2}{2m} \right)^2 \sum_\sigma \exp \left(-2z \sqrt{\frac{2m\Phi_\sigma}{\hbar^2}} \right) N_t^\sigma(E_F) \int dE [f(E - eV) - f(E)] g_s^\sigma(E) \quad (4)$$

where Φ_σ is the average of sample and tip work functions (which is assumed to be large in comparison with eV for simplicity), z is the distance between the surface and the tip. Here $N_t(E)$ is the density of states (DOS) of the tip material, which is supposed to be smooth and thus is replaced by its value at the Fermi energy, and

$$g_s^\sigma(E) = \sum_\nu \mathcal{A}_\nu^\sigma(E) \langle \nu\sigma | \delta(\mathbf{k}_\parallel) | \nu\sigma \rangle \quad (5)$$

is the density of states of the sample with zero in-plane component of the wave-vector: $\mathbf{k}_\parallel = 0$ so that the summation is performed only over two points of the Fermi surface. This condition means that the tunneling probability has a sharp (at not too small z) maximum for the states with velocity direction normal to the surface. For a generic multi-sheet Fermi surfaces the condition of the dominant tunneling is, generally speaking, more complicated, but this modifies only some weakly bias-dependent factors.

III. NON-QUASIPARTICLE STATES IN INHOMOGENEOUS MATERIALS

Since STM probes only surface one has to discuss first modification of NQP states in comparison with the case of ideal bulk crystal. The existence of NQP states at the surface of HMF has been demonstrated for a narrow-band Hubbard model [28]. Here we present a general derivation valid in the case of arbitrary inhomogeneity.

To describe the effects of electron-magnon interaction for the inhomogeneous case we use the formalism of the exact eigenfunctions developed earlier for the impurity-state problem in a ferromagnetic semiconductor [29]. The corresponding Hamiltonian of the $s-d$ exchange model reads

$$\begin{aligned}\mathcal{H} &= \int d\mathbf{r} \left(\sum_{\sigma} \Psi_{\sigma}^{\dagger}(\mathbf{r}) \mathcal{H}_0^{\sigma} \Psi_{\sigma}(\mathbf{r}) - I \sum_{\sigma\sigma'} \delta\mathbf{S}(\mathbf{r}) \Psi_{\sigma}^{\dagger}(\mathbf{r}) \boldsymbol{\sigma}_{\sigma\sigma'} \Psi_{\sigma'}(\mathbf{r}) \right) + \mathcal{H}_d \\ \mathcal{H}_0^{\sigma} &= -\frac{\hbar^2}{2m} \nabla^2 + U_{\sigma}(\mathbf{r})\end{aligned}\quad (6)$$

where $U_{\sigma}(\mathbf{r})$ is the potential energy (with account of the electron-electron interaction in the mean field approximation) which is supposed to be spin dependent, $\Psi_{\sigma}(\mathbf{r})$ is the field operator for the spin projection σ , $\mathbf{S}(\mathbf{r})$ is the spin density of the localized-moment system, $\delta\mathbf{S}(\mathbf{r}) = \mathbf{S}(\mathbf{r}) - \langle\mathbf{S}(\mathbf{r})\rangle$ is its fluctuating part, the effect of the average spin polarization $\langle\mathbf{S}(\mathbf{r})\rangle$ being included into $U_{\sigma}(\mathbf{r})$. We use an approximation of contact electron-magnon interaction described by the $s-d$ exchange parameter I ,

$$\mathcal{H}_d = - \sum_{\mathbf{q}} J_{\mathbf{q}} \mathbf{S}_{\mathbf{q}} \mathbf{S}_{-\mathbf{q}} \quad (7)$$

is the Heisenberg Hamiltonian of localized spin (for simplicity we neglect the inhomogeneity effects for the magnon subsystem).

Passing to the representation of the exact eigenfunctions of the Hamiltonian \mathcal{H}_0^{σ} ,

$$\begin{aligned}\mathcal{H}_0^{\sigma} \psi_{\nu\sigma} &= \varepsilon_{\nu\sigma} \psi_{\nu\sigma}, \\ \Psi_{\sigma}(\mathbf{r}) &= \sum_{\nu} \psi_{\nu\sigma}(\mathbf{r}) c_{\nu\sigma},\end{aligned}\quad (8)$$

one can rewrite the Hamiltonian (6) in the following form:

$$\mathcal{H} = \sum_{\nu\sigma} \varepsilon_{\nu\sigma} c_{\nu\sigma}^{\dagger} c_{\nu\sigma} - I \sum_{\mu\nu\alpha\beta\mathbf{q}} (\nu\alpha, \mu\beta|\mathbf{q}) \delta\mathbf{S}_{\mathbf{q}} c_{\nu\alpha}^{\dagger} \boldsymbol{\sigma}_{\alpha\beta} c_{\mu\beta} + \mathcal{H}_d \quad (9)$$

where

$$(\nu\sigma, \mu\sigma'|\mathbf{q}) = \langle\mu\sigma'| e^{i\mathbf{q}\mathbf{r}} |\nu\sigma\rangle.$$

We take into account again the electron-spectrum spin splitting in the mean-field approximation by keeping the dependence of the eigenfunctions on the spin projection.

We restrict ourselves to the spin-wave region where we can use for the spin operators the magnon (e.g., Dyson-Maleev) representation. Then we have for the one-electron Green's function

$$G_{\nu}^{\sigma}(E) = [E - \varepsilon_{\nu\sigma} - \Sigma_{\nu}^{\sigma}(E)]^{-1}, \quad (10)$$

with the self-energy $\Sigma_{\nu}^{\sigma}(E)$ describing correlation effects.

We start with the perturbation expansion in the electron-magnon interaction. To second order in I one has

$$\Sigma_{\nu}^{\sigma}(E) = 2I^2 S Q_{\nu}^{\sigma}(E) \quad (11)$$

with

$$Q_{\nu}^{\uparrow}(E) = \sum_{\mu\mathbf{q}} |(\nu\uparrow, \mu\downarrow|\mathbf{q})|^2 \frac{N_{\mathbf{q}} + n_{\mu}^{\downarrow}}{E - \varepsilon_{\mu\downarrow} + \omega_{\mathbf{q}}}, \quad Q_{\nu}^{\downarrow}(E) = \sum_{\mu\mathbf{q}} |(\nu\downarrow, \mu\uparrow|\mathbf{q})|^2 \frac{1 + N_{\mathbf{q}} - n_{\mu}^{\uparrow}}{E - \varepsilon_{\mu\uparrow} - \omega_{\mathbf{q}}} \quad (12)$$

where $n_{\mu}^{\sigma} = f(\varepsilon_{\mu\sigma})$, $\omega_{\mathbf{q}}$ is the magnon energy, $N_{\mathbf{q}} = N_B(\omega_{\mathbf{q}})$ is the Bose function.

Using the expansion of the Dyson equation (10) we obtain for the spectral density

$$\begin{aligned}\mathcal{A}_{\nu\sigma}(E) &= -\frac{1}{\pi} \text{Im} G_{\nu}^{\sigma}(E) = \delta(E - \varepsilon_{\nu\sigma}) \\ &\quad - \delta'(E - \varepsilon_{\nu\sigma}) \text{Re} \Sigma_{\nu}^{\sigma}(E) - \frac{1}{\pi} \frac{\text{Im} \Sigma_{\nu}^{\sigma}(E)}{(E - \varepsilon_{\nu\sigma})^2}\end{aligned}\quad (13)$$

The second term in the right-hand side of Eq.(13) gives the shift of quasiparticle energies. The third term, which arises from the branch cut of the self-energy, describes the incoherent (non-quasiparticle) contribution owing to scattering by magnons. One can see that this does not vanish in the energy region, corresponding to the “alien” spin subband with the opposite projection $-\sigma$.

Neglecting temporarily in Eq.(12) the magnon energy $\omega_{\mathbf{q}}$ in comparison with typical electron energies and using the identities

$$\begin{aligned} \sum_{\mu \mathbf{q}} \frac{|\langle \nu \mu | \mathbf{q} \rangle|^2}{E - \varepsilon_{\mu}} F(\varepsilon_{\mu}) &= -\frac{1}{\pi} \int dE' \frac{F(E')}{E - E'} \text{Im} \sum_{\mu \mathbf{q}} \frac{|\langle \nu \mu | \mathbf{q} \rangle|^2}{E' - \varepsilon_{\mu} + i0} \\ &= -\frac{1}{\pi} \int dE' \frac{F(E')}{E - E'} \text{Im} \sum_{\mathbf{q}} \langle \nu | e^{i\mathbf{q}\mathbf{r}} (E' - \mathcal{H}_0 + i0)^{-1} e^{-i\mathbf{q}\mathbf{r}} | \nu \rangle \\ &= -\frac{1}{\pi} \int dE' \frac{F(E')}{E - E'} \text{Im} \langle \nu | (E' - \mathcal{H}_0 + i0)^{-1} | \nu \rangle \end{aligned} \quad (14)$$

we derive

$$\Sigma_{\nu}^{\uparrow}(E) = 2I^2 S \int dE' f(E') \langle \nu \uparrow | \delta(E - E' - \mathcal{H}_0^{\downarrow}) | \nu \uparrow \rangle \quad (15)$$

$$\Sigma_{\nu}^{\downarrow}(E) = 2I^2 S \int dE' [1 - f(E')] \langle \nu \downarrow | \delta(E - E' - \mathcal{H}_0^{\uparrow}) | \nu \downarrow \rangle \quad (16)$$

Here we restrict ourselves only to the case of zero temperature $T = 0$ neglecting the magnon occupation numbers $N_{\mathbf{q}}$. Using the tight-binding model for the ideal-crystal Hamiltonian we find in the real-space representation

$$\Sigma_{\mathbf{R},\mathbf{R}'}^{\uparrow}(E) = 2I^2 S \int dE' f(E') \left(-\frac{1}{\pi} \text{Im} G_{\mathbf{R},\mathbf{R}}^{\downarrow}(E') \right) \delta_{\mathbf{R},\mathbf{R}'} \quad (17)$$

$$\Sigma_{\mathbf{R},\mathbf{R}'}^{\downarrow}(E) = 2I^2 S \int dE' [1 - f(E')] \left(-\frac{1}{\pi} \text{Im} G_{\mathbf{R},\mathbf{R}}^{\uparrow}(E') \right) \delta_{\mathbf{R},\mathbf{R}'} \quad (18)$$

where \mathbf{R}, \mathbf{R}' are lattice site indices, and therefore

$$\Sigma_{\nu}^{\sigma}(E) = \sum_{\mathbf{R}} |\psi_{\nu\sigma}(\mathbf{R})|^2 \Sigma_{\mathbf{R},\mathbf{R}}^{\sigma}(E). \quad (19)$$

Following the method developed by us earlier [12, 29] one can generalize the above results to the case of arbitrary $s-d$ exchange parameter. Simplifying the sequence of equations of motion (cf. Ref.29) we obtain the integral equation

$$(E - \varepsilon_{\nu\sigma}) G_{\nu\lambda}^{\sigma}(E) = \delta_{\nu\lambda} + \sigma I R_{\nu\lambda}^{\sigma}(E) - \sigma I \sum_{\kappa} (E - \varepsilon_{\kappa-\sigma}) R_{\kappa\lambda}^{\sigma}(E) G_{\nu\kappa}^{\sigma}(E) \quad (20)$$

where

$$\begin{aligned} R_{\nu\lambda}^{\uparrow}(E) &= \sum_{\mu \mathbf{q}} (\mu \downarrow, \lambda \uparrow | -\mathbf{q}) (\nu \uparrow, \mu \downarrow | \mathbf{q}) \frac{n_{\mu}^{\downarrow}}{E - \varepsilon_{\mu\downarrow} + \omega_{\mathbf{q}}}, \\ R_{\nu\lambda}^{\downarrow}(E) &= \sum_{\mu \mathbf{q}} (\mu \uparrow, \lambda \downarrow | \mathbf{q}) (\nu \downarrow, \mu \uparrow | \mathbf{q}) \frac{1 - n_{\mu}^{\uparrow}}{E - \varepsilon_{\mu\uparrow} - \omega_{\mathbf{q}}} \end{aligned} \quad (21)$$

Note that the equation (20) is exact in the case of empty conduction band ($n_{\nu\sigma} = 0$, one current carrier, ferromagnetic semiconductor situation), and for finite band filling this corresponds to a ladder approximation in the diagram approach.

Similar to (14), we obtain after neglecting the magnon energies in (21) the equation for the Green' function

$$\sum_{\kappa} (E - \varepsilon_{\kappa-\sigma}) R_{\kappa\lambda}^{\sigma}(E) G_{\nu\kappa}^{\sigma}(E) = \langle \nu \sigma | R^{\sigma}(E) (E - \mathcal{H}_0^{\sigma} + i0)^{-1} G^{\sigma}(E) | \nu \sigma \rangle \quad (22)$$

where we use the matrix notations. Then we have for the operator Green' function

$$G^{\sigma}(E) = \left[E - \mathcal{H}_0^{\sigma} + \sigma I (\mathcal{H}_0^{\sigma} - \mathcal{H}_0^{-\sigma}) \frac{1}{1 + \sigma I R^{\sigma}(E)} R^{\sigma}(E) \right]^{-1} \quad (23)$$

If we consider spin dependence of electron spectrum in the simplest rigid-splitting approximation $\varepsilon_{\nu\sigma} = \varepsilon_\nu - \sigma I \langle S^z \rangle$ and thus neglect spin-dependence of the eigenfunctions $\psi_{\nu\sigma}(\mathbf{R})$ the expressions (15),(16) are drastically simplified. Then the self-energy does not depend on ν and we have

$$\Sigma^\sigma(E) = \frac{2I^2 S R^\sigma(E)}{1 + \sigma I R^\sigma(E)}, \quad (24)$$

$$R^\uparrow(E) = \sum_\mu \frac{n_\mu^\downarrow}{E - \varepsilon_{\mu\downarrow}}, \quad R^\downarrow(E) = \sum_\mu \frac{1 - n_\mu^\uparrow}{E - \varepsilon_{\mu\uparrow}} \quad (25)$$

If \mathcal{H}_0^σ is just the crystal Hamiltonian ($\nu = \mathbf{k}, \varepsilon_{\nu\sigma} = t_{\mathbf{k}\sigma}$, $t_{\mathbf{k}\sigma}$ being the band energy), the expression (23) coincides with that obtained in Ref. 12 for the Hubbard model after the replacement $I \rightarrow U$.

The expression (23) can be also represented in the form

$$G^\sigma(E) = \left[E - \mathcal{H}_0^{-\sigma} - (\mathcal{H}_0^\sigma - \mathcal{H}_0^{-\sigma}) \frac{1}{1 + \sigma I R^\sigma(E)} \right]^{-1} \quad (26)$$

The equation (26) is convenient in the narrow-band case. In this limit where spin splitting is large in comparison with the bandwidth of conduction electrons we have $\mathcal{H}_0^\uparrow - \mathcal{H}_0^\downarrow = -2IS$ and we obtain for the “lower” spin subband with $\sigma = -\text{sign}I$

$$G^\sigma(E) = \left[E - \mathcal{H}_0^{-\sigma} + \frac{2S}{R^\sigma(E)} \right]^{-1} \quad (27)$$

For a periodic crystal Eq.(27) takes the form

$$G_{\mathbf{k}}^\sigma(E) = \left[E - t_{\mathbf{k}-\sigma} + \frac{2S}{R^\sigma(E)} \right]^{-1} \quad (28)$$

This expression yields exact result in the limit $I \rightarrow +\infty$,

$$G_{\mathbf{k}}^\downarrow(E) = \left[\epsilon - t_{\mathbf{k}} + \frac{2S}{R(\epsilon)} \right]^{-1}, \quad R(\epsilon) = \sum_{\mathbf{k}} \frac{1 - f(t_{\mathbf{k}})}{\epsilon - t_{\mathbf{k}}} \quad (29)$$

with $\epsilon = E + IS$, $t_{\mathbf{k}}$ the bare electron spectrum. In the limit $I \rightarrow -\infty$ Eq.(28) gives correctly the spectrum of spin-down quasiparticles,

$$G_{\mathbf{k}}^\downarrow(E) = \frac{2S}{2S+1} [\epsilon - t_{\mathbf{k}}^*]^{-1} \quad (30)$$

with $\epsilon = E - I(S+1)$, $t_{\mathbf{k}}^* = [2S/(2S+1)]t_{\mathbf{k}}$. However, it does not describe the NQP states quite correctly, so that more accurate expressions can be obtained by using the atomic representation [30],

$$G_{\mathbf{k}}^\uparrow(E) = \frac{2S}{2S+1} \left[\epsilon - t_{\mathbf{k}}^* + \frac{2S}{R^*(\epsilon)} \right]^{-1}, \quad R^*(\epsilon) = \sum_{\mathbf{k}} \frac{f(t_{\mathbf{k}}^*)}{\epsilon - t_{\mathbf{k}}^*} \quad (31)$$

On the other hand, the result (27), (28) yields a good interpolation description in the Hubbard model [9, 10, 12].

The Green's functions (28), (29), (31) have no poles, at least for small current carrier concentration, and the whole spectral weight of minority states is provided by the branch cut (non-quasiparticle states) [10, 12]. For surface states this result was obtained in Ref.28 in a narrow-band Hubbard model. Now we see that this result can be derived in an arbitrary inhomogeneous case. For a HMF with the gap in the minority spin subband NQP states occur above the Fermi level, and for the gap in the majority spin subband below the Fermi level.

In the absence of spin dynamics (i.e., neglecting the magnon frequencies) the NQP density of states has a jump at the Fermi level. However, the magnon frequencies can be restored in the final result, in analogy with the case of ideal crystal, which leads to a smearing of the jump on the energy scale of a characteristic magnon energy $\overline{\omega}$. It should be mentioned once more that we restrict ourselves to the case of the usual three-dimensional magnon spectrum and do not consider the influence of surface states on the spin-wave subsystem. The expressions obtained enable us to investigate the energy dependence of the spectral density.

IV. THE NON-QUASIPARTICLE DENSITY OF STATES

An analysis of the electron-spin coupling yields different pictures for two possible signs of the $s - d$ exchange parameter I . For $I > 0$ the spin-down NQP scattering states form a “tail” of the upper spin-down band, which starts from E_F (Fig.1) since the Pauli principle prevents electron scattering into occupied states.

For $I < 0$ spin-up NQP states are present below the Fermi level as an isolated region (Fig.2): occupied states with the total spin $S - 1$ are a superposition of the states $|S\rangle|\downarrow\rangle$ and $|S - 1\rangle|\uparrow\rangle$. The entanglement of the states of electron and spin subsystems which is necessary to form the NQP states is a purely quantum effect formally disappearing at $S \rightarrow \infty$. To understand better why the NQP states are formed only below E_F in this case we can treat the limit $I = -\infty$. Then the current carrier is really a many-body state of the occupied site as a whole with total spin $S - 1/2$, which propagates in the ferromagnetic medium with spin S at any site. The fractions of the states $|S\rangle|\downarrow\rangle$ and $|S - 1\rangle|\uparrow\rangle$ in the current carrier state are $1/(2S + 1)$ and $2S/(2S + 1)$, respectively, so that the first number is just a spectral weight of occupied spin-up electron NQP states. At the same time, the density of empty states is measured by the number of electrons with a given spin projection which one can add to the system. It is obvious that one cannot put any spin-up electrons in the spin-up site at $I = -\infty$. Therefore the density of NQP states should vanish above E_F .

It is worthwhile to note that in the most of known HMF the gap exists for minority-spin states [2]. This is similar to the case $I > 0$, so that the NQP states should arise above the Fermi energy. For exceptional cases with the majority-spin gap such as a double perovskite $\text{Sr}_2\text{FeMoO}_6$ [31] one should expect formation of the NQP states below the Fermi energy.

It has been proven in the previous section that the presence of space inhomogeneity (e.g., surface) does not change qualitatively the spectral density picture, except smooth matrix elements. Therefore further in this section we will consider, for simplicity, the case of clean infinite crystal; all the temperature and energy dependences of the spectral density will be basically the same for the surface layer.

The second term in the right-hand side of Eq. (13) describes the renormalization of quasiparticle energies. The third term, which arises from the branch cut of the self-energy $\Sigma_{\nu\sigma}(E)$, describes the incoherent (non-quasiparticle) contribution owing to scattering by magnons. One can see that this does not vanish in the energy region, corresponding to the “alien” spin subband with the opposite projection $-\sigma$. Further on we perform for definiteness concrete calculations in the case $I > 0$ (the case $I < 0$ differs, roughly speaking, by a particle-hole transformation). Summing up Eq.(13) to find the total DOS $N_\sigma(E)$ and neglecting the quasiparticle shift we obtain

$$\begin{aligned} N_\uparrow(E) &= \sum_{\mathbf{k}\mathbf{q}} \left[1 - \frac{2I^2 S N_{\mathbf{q}}}{(t_{\mathbf{k}+\mathbf{q}\downarrow} - t_{\mathbf{k}\uparrow})^2} \right] \delta(E - t_{\mathbf{k}\uparrow}) \\ N_\downarrow(E) &= 2I^2 S \sum_{\mathbf{k}\mathbf{q}} \frac{1 + N_{\mathbf{q}} - n_{\mathbf{k}\uparrow}}{(t_{\mathbf{k}+\mathbf{q}\downarrow} - t_{\mathbf{k}\uparrow} - \omega_{\mathbf{q}})^2} \delta(E - t_{\mathbf{k}\uparrow} - \omega_{\mathbf{q}}) \end{aligned} \quad (32)$$

where we consider for simplicity only second-order perturbation expression. Basing on a general consideration in the previous section one can prove that, actually, this expression holds for arbitrary I , at least, in the framework of $1/2S$ expansion.

The $T^{3/2}$ -dependence of the magnon contribution to the residue of the Green’s function, i.e. of the effective electron mass in the lower spin subband, and an increase with temperature of the incoherent tail from the upper spin subband result in a strong temperature dependence of partial densities of states $N_\sigma(E)$, the corrections being of opposite sign. At the same time, the temperature shift of the band edge for the quasiparticle states is proportional to $T^{5/2}$ rather than to magnetization [10, 29].

The exact solution in the atomic limit (for one conduction electron), which is valid not only in spin-wave region, but for arbitrary temperatures, reads [32]

$$G^\sigma(E) = \frac{S + 1 + \sigma \langle S^z \rangle}{2S + 1} \frac{1}{E + IS} + \frac{S - \sigma \langle S^z \rangle}{2S + 1} \frac{1}{E - I(S + 1)}. \quad (33)$$

In this case the energy levels are not temperature dependent at all, whereas the residues are strongly temperature dependent via the magnetization.

Now we consider the case $T = 0$ for a finite band filling. The picture of $N(E)$ in HMF (or degenerate ferromagnetic semiconductor) demonstrates strong energy dependence near the Fermi level (Figs. 1,2). If we neglect magnon frequencies in the denominators of Eq.(32), the partial density of incoherent states should occur by a jump above or below the Fermi energy E_F for $I > 0$ and $I < 0$ respectively owing to the Fermi distribution functions. An account of finite magnon frequencies $\omega_{\mathbf{q}} = \mathcal{D}q^2$ (\mathcal{D} is the spin wave stiffness constant) leads to smearing of these singularities, $N(E_F)$ being equal to zero. For $|E - E_F| \ll \varpi$ we obtain

$$\frac{N_{-\alpha}(E)}{N_{\alpha}(E)} = \frac{1}{2S} \left| \frac{E - E_F}{\bar{\omega}} \right|^{3/2} \theta(\alpha(E - E_F)), \alpha = \text{sgn} I \quad (34)$$

($\alpha = \pm$ corresponds to the spin projections \uparrow, \downarrow). With increasing $|E - E_F|$, $N_{-\alpha}/N_{\alpha}$ tends to a constant value which is of order of I^2 within the perturbation theory.

In the strong coupling limit where $|I| \rightarrow \infty$ we have from (32)

$$\frac{N_{-\alpha}(E)}{N_{\alpha}(E)} = \frac{1}{2S} \theta(\alpha(E - E_F)), |E - E_F| \gg \bar{\omega} \quad (35)$$

In fact, this expression is valid only in the framework of the $1/2S$ -expansion, and in the narrow-band quantum case we have to use more exact expressions (29),(31). In numerical calculations, we follow to Ref.30 and smear the resolvents,

$$R(E) \rightarrow \bar{R}(E) = \int d\omega K(\omega) R(E \pm \omega)$$

We use the semielliptic magnon DOS $K(\omega)$ which is proportional (with the corresponding shift) to the bare electron DOS, the maximum magnon frequency being determined by the electron concentration c [30]. This approximation provides the correct behavior near the Fermi level (cf. Ref.33), although gives an unphysical shift of the band bottom by the maximum magnon frequency.

The results of calculations are shown in Figs.3, 4. One can see that in the model with $I \rightarrow -\infty$ (for $S = 1/2$ this is equivalent to the Hubbard model with the replacement $t_{\mathbf{k}} \rightarrow t_{\mathbf{k}}/2$, see Refs.10, 12) the “Kondo” peaks [33] modify considerably the picture. Note that the function $-(1/\pi)\text{Im}\bar{R}^*(E)$, which yields DOS in the lowest-order approximation in the electron concentration, does not have such peaks.

To investigate details of the energy dependence of $N(E)$ in the broad-band case we assume the simplest isotropic approximation for the majority-spin electrons,

$$t_{\mathbf{k}\uparrow} - E_F \equiv \xi_{\mathbf{k}} = \frac{k^2 - k_F^2}{2m^*}. \quad (36)$$

Provided that we use the rigid splitting approximation $t_{\mathbf{k}\downarrow} = t_{\mathbf{k}\uparrow} + \Delta$ ($\Delta = 2IS, I > 0$), the half-metallic situation (or, more precisely, the situation of degenerate ferromagnetic semiconductor) takes place for $\Delta > E_F$. Then qualitatively the equation (34) works to accuracy of a prefactor. It is worthwhile to note that, formally speaking, the NQP contribution to DOS occurs also for an “usual” metal where $\Delta < E_F$. In the case of small Δ there is a crossover energy (or temperature) scale

$$T^* = \mathcal{D}(m^* \Delta / k_F)^2 \quad (37)$$

which is the magnon energy at the boundary of Stoner continuum, $T^* \simeq \bar{\omega}(\Delta/E_F)^2 \ll \bar{\omega}$. At $|E - E_F| \ll \bar{\omega}$ the equation (32) for the NQP contribution reads

$$\delta N_{\downarrow}(E) \propto \left[\frac{1}{2} \ln \left| \frac{1 + \sqrt{(E - E_F)/T^*}}{1 - \sqrt{(E - E_F)/T^*}} \right| - \sqrt{(E - E_F)/T^*} \right] \theta(E - E_F). \quad (38)$$

At $|E - E_F| \ll T^*$ this gives the same results as above. However, at $T^* \ll |E - E_F| \ll \bar{\omega}$ this contribution is proportional to $-\sqrt{(E - E_F)/T^*}$ and is *negative* (of course, the total DOS is always positive). This demonstrates that one should be very careful when discussing the NQP states for the systems which are not half-metallic.

The model of rigid spin splitting used above is in fact not applicable for the real HMF where the gap has a hybridization origin [1, 2]. The simplest model for HMF is as follows: a “normal” metallic spectrum for majority electrons (36) and the hybridization gap for minority ones,

$$t_{\mathbf{k}\downarrow} - E_F = \frac{1}{2} \left(\xi_{\mathbf{k}} + \text{sgn}(\xi_{\mathbf{k}}) \sqrt{\xi_{\mathbf{k}}^2 + \Delta^2} \right) \quad (39)$$

Here we assume for simplicity that the Fermi energy lies exactly in the middle of the hybridization gap (otherwise one needs to shift $\xi_{\mathbf{k}} \rightarrow \xi_{\mathbf{k}} + E_0 - E_F$ in the last equation, E_0 being the middle of the gap). One can replace in Eq.(32) $\xi_{\mathbf{k}+\mathbf{q}}$ by $\mathbf{v}_{\mathbf{k}}\mathbf{q}$, $\mathbf{v}_{\mathbf{k}} = \mathbf{k}/m^*$. First, we integrate over the angle between the vectors \mathbf{k} and \mathbf{q} . It is easy to calculate

$$\left\langle \left(\frac{1}{t_{\mathbf{k}+\mathbf{q}\downarrow} - t_{\mathbf{k}\uparrow} - \omega_{\mathbf{q}}} \right)^2 \right\rangle = \frac{8}{v_F q \Delta} \left(\frac{2}{3} \left[X^3 - (X^2 + 1)^{3/2} + 1 \right] + X \right) \quad (40)$$

where angular brackets stand for the average over the angles of the vector \mathbf{k} , $X = k_F q / m^* \Delta$. Here we do have the crossover with the energy scale T^* which can be small for small enough hybridization gap. For example, in NiMnSb the conduction band width is about 5 eV and the distance from the Fermi level to the nearest gap edge (i.e. indirect energy gap which is proportional to Δ^2) is smaller than 0.5 eV, so that $(\Delta/E_F)^2 \leq 0.1$.

For the case $0 < E - E_F \ll \bar{\omega}$ one has

$$N_{\downarrow}(E) \propto b\left(\frac{E - E_F}{T^*}\right), b(y) = \frac{2}{5} \left[y^{5/2} - (1+y)^{5/2} + 1 \right] + y + y^{3/2} = \begin{cases} y^{3/2}, & y \ll 1 \\ y, & y \gg 1 \end{cases} \quad (41)$$

The function $b(x)$ is shown in Fig.5. Thus the behavior $N_{\downarrow}(E) \propto (E - E_F)^{3/2}$ takes place only for very small excitation energies $E - E_F \ll T^*$, whereas in a broad interval $T^* \ll E - E_F \ll \bar{\omega}$ one has the linear dependence $N_{\downarrow}(E) \propto E - E_F$.

V. THE TEMPERATURE DEPENDENCE OF SPIN POLARIZATION

Simple qualitative considerations [34], as well as direct Green's functions calculations [11, 35] for magnetic semiconductors, demonstrate that spin polarization of conduction electrons in the spin-wave region is proportional to magnetization

$$P \equiv \frac{N_{\uparrow} - N_{\downarrow}}{N_{\uparrow} + N_{\downarrow}} = 2P_0 \langle S^z \rangle \quad (42)$$

A weak ground-state depolarization $1 - P_0$ occurs in the case where $I > 0$. The behavior $P(T) \simeq \langle S^z \rangle$ is qualitatively confirmed by experimental data on field emission from ferromagnetic semiconductors [36] and transport properties of half-metallic Heusler alloys [37].

An attempt was used [38] to generalize the result (42) on the HMF case (in fact, using qualitative arguments which are valid only in the atomic limit, see Eq.(33)). However, we will demonstrate that the situation for HMF is more complicated.

In this section we focus on the magnon contribution to DOS (32) and calculate the function

$$\Lambda = \sum_{\mathbf{k}\mathbf{q}} \frac{2I^2 S N_{\mathbf{q}}}{(t_{\mathbf{k}+\mathbf{q}\downarrow} - t_{\mathbf{k}\uparrow} - \omega_{\mathbf{q}})^2} \delta(E_F - t_{\mathbf{k}\uparrow}) \quad (43)$$

Using the parabolic electron spectrum $t_{\mathbf{k}\uparrow} = k^2/2m^*$ and averaging over the angles of the vector \mathbf{k} we obtain

$$\Lambda = \frac{2I^2 S m^2}{k_F^2} \rho \sum_{\mathbf{q}} \frac{N_{\mathbf{q}}}{(q^*)^2 - q^2} \quad (44)$$

where $\rho = N_{\uparrow}(E_F, T=0)$, we have used the condition $q \ll k_F$, $q^* = m^* \Delta / k_F = \Delta / v_F$, where $\Delta = 2|I|S$ is the spin splitting. In the ferromagnetic semiconductor we have, in agreement with the qualitative considerations presented above:

$$\Lambda = \frac{S - \langle S^z \rangle}{2S} \rho \propto \left(\frac{T}{T_C} \right)^{3/2} \rho \quad (45)$$

Further on we consider the spectrum model (36), (39) where the gap has a hybridization origin. At $T \ll T^*$ we reproduce the result (45) which is actually universal for this temperature region. At $T^* \ll T \ll \bar{\omega}$ we derive

$$\Lambda = \sum_{\mathbf{k}\mathbf{q}} 2I^2 S N_{\mathbf{q}} \delta(\xi_{\mathbf{k}}) \frac{16}{3v_F q \Delta} \propto q^* \sum_{\mathbf{q}} \frac{N_{\mathbf{q}}}{q} \propto \frac{T^{*1/2}}{T_C^{1/2}} T \ln \frac{T}{T^*} \quad (46)$$

This result distinguishes HMF like the Heusler alloys from ferromagnetic semiconductors and narrow-band saturated ferromagnets. In the narrow-band case the spin polarization follows the magnetization up to the Curie temperature T_C .

For finite temperatures the density of NQP states at the Fermi energy is proportional to [11, 23, 34]

$$N(E_F) \propto \int_0^\infty d\omega \frac{K(\omega)}{\sinh(\omega/T)} \quad (47)$$

Generally, for temperatures which are comparable with the Curie temperature T_C there are no essential difference between half-metallic and “ordinary” ferromagnets since the gap is filled. The corresponding symmetry analysis is performed in Ref. 23 for a model of conduction electrons interacting with “pseudospin” excitations in ferroelectric semiconductors. The symmetrical (with respect to E_F) part of $N(E)$ in the gap can be attributed to smearing of electron states by electron-magnon scattering; the asymmetrical (“Kondo-like”) one is the density of NQP states owing to the Fermi distribution function. Note that this filling of the gap is very important for possible applications of HMF in spintronics: they really have some advantages only provided that $T \ll T_C$. Since a single-particle Stoner-like theory leads to much less restrictive (but unfortunately completely wrong) inequality $T \ll \Delta$, the many-body treatment of the spin-polarization problem (inclusion of collective spin-wave excitations) is required.

VI. BIAS DEPENDENCE OF THE TUNNELING CONDUCTANCE

Now we consider an application of the results obtained above to the tunneling spectroscopy problem. The formulas of Sect.4 for the energy dependence of NQP contributions are, strictly speaking, derived for the usual one-electron density of states at E_F , which is observed, say, in photoemission measurements. However, the factor of $g_s^\sigma(E)$, which is present in the expression for the tunneling current (4), does not influence the temperature dependence, and therefore these results are valid for spin polarization from tunneling conductance at zero bias in STM.

The only difference in the NQP contributions to $g_s^\sigma(E)$ and $N_\sigma(E)$ is in that after summation over the magnon wavevector \mathbf{q} the integration is performed over not in the whole Fermi surface, but its two points (see Eq.(5)). For a spherical Fermi surface for majority electrons the results differ by the constant factor of the Fermi surface diameter. However, the energy and temperature dependences should be the same in a more general case.

Consider the bias dependence of the tunneling current for zero temperature. One can see from Eq.(4) that

$$\frac{d\mathcal{I}^\sigma(V)}{dV} \propto g_s^\sigma(eV) \propto N_\sigma(eV) \quad (48)$$

Again, the last proportionality can be strictly justified in the case of a spherical Fermi surface only, but is qualitatively valid for arbitrary electron spectrum.

One should keep in mind that sometimes the surface of HMF is not half-metallic; in particular, this is the case of a prototype HMF, NiMnSb [39]. In such a situation, the tunneling current for minority electrons is due to the surface states only. However, the NQP states can be still visible in the tunneling current via the hybridization of the bulk states with the surface one. The hybridization lead to the Fano antiresonance picture which is usually observed in STM investigations of the Kondo effect at metallic surfaces (see, e.g., Refs. 40, 41, 42). In these cases the tunneling conductance will be proportional to a mixture of $N_\sigma(eV)$ and $L_\sigma(eV)$, $L_\sigma(E)$ being the real part of the on-site Green’s function,

$$L_\sigma(E) = \mathcal{P} \int dE' \frac{N_\sigma(E')}{E - E'}. \quad (49)$$

(\mathcal{P} stands for principal value, E is referred to the Fermi energy). Surprisingly, in this case the effect of NQP states on the tunneling current can be even more pronounced in comparison with the ideal crystal. The reason is that the analytical continuation of the jump in $N_\sigma(E)$ is logarithm; both singularities are cut at the energy $\bar{\omega}$; nevertheless, the energy dependence of $L_\sigma(E)$ can be pronounced, see Fig.6. This is similar to the effect of enhancement of the NQP contribution to the x-ray absorption and emission spectra, which was predicted in Ref. 15.

Now we discuss in more detail the energy dependence for $|E| \ll \bar{\omega}$. The analytical continuation of the $E^{3/2}\theta(E)$ -contribution to $N_\sigma(E)$ yields the contribution $(-E)^{3/2}\theta(-E)$ in $L_\sigma(E)$ which is non-zero on the other side with respect to E_F (a situation that is formally similar to the electronic topological transition, see Ref.46). The one-sided linear dependence in $N_\sigma(E)$ according to Eq.(41) corresponds to $E \ln |E|$ in $L_\sigma(E)$.

STM measurements of electron DOS give also an opportunity to probe *bosonic* excitations interacting with the conduction electrons. Due to electron-phonon coupling, the derivative $dN_\sigma(E)/dE$ and thus $d^2\mathcal{I}^\sigma(V)/dV^2$ at $eV = E$ have peaks at the energies $E = \pm\omega_i$ corresponding to the peaks in the phonon DOS. According to our results (see, e.g., Eq.(32), the same effect should be observable for the case of electron-magnon interaction. However, in the latter case these peaks are essentially asymmetric with respect to the Fermi energy (zero bias) due to asymmetry of the non-quasiparticle contributions. This asymmetry can be used to distinguish phonon and magnon peaks.

VII. CONCLUSIONS

In the present paper we have demonstrated that non-quasiparticle states in half-metallic ferromagnets exist not only for an ideal crystal, but also in the presence of an arbitrary external potential. In particular, they occur at the surface of the half-metallic ferromagnets. These states can be probed by the STM both directly and via their effect on the surface states (the Fano antiresonance case). Therefore, they can be observable even for the situation of surface “dead layers” where the surface is not half-metallic. The expressions obtained can be used for realistic electronic structure calculations of NQP contributions to the electron energy spectrum of the surfaces of HMF.

Temperature dependence of the spin polarization at the Fermi energy which can be also probed by the STM follows the temperature dependence of magnetization at very low temperatures. For the HMF with a hybridization gap, there is a crossover energy (temperature) $T^* \ll T_C$ where the character of the temperature dependence is changed. The energy dependence of the NQP contributions (and consequently the bias dependence of the tunneling current) is strongly influenced by the band structure too. In particular, for HMF with a hybridization gap this demonstrates a linear rather than $E^{3/2}$ behavior in a wide interval. In the narrow-band case a Kondo-like peak (Fig.4) near the Fermi level should be observed in tunneling experiments.

Due to asymmetry of NQP states with respect to the Fermi energy, the magnon peaks in $d^2\mathcal{I}^\sigma(V)/dV^2$ are also asymmetric with respect to the zero bias, in contrast with the phonon ones. This gives an opportunity to distinguish between phonon and magnon peaks in the inelastic spectroscopy by STM.

In principle, the NQP effects discussed should exist also in usual metallic ferromagnets. However, only in HMF they can be picked up in a pure form.

The research described was supported in part by Grant No. 747.2003.2 (Support of Scientific Schools) from the Russian Basic Research Foundation and by the Netherlands Organization for Scientific Research (Grant NWO 047.016.005).

-
- [*] E-mail: Valentin.Irkhin@imp.uran.ru
- [1] R. A. de Groot, F. M. Müller, P. G. van Engen, and K. H. J. Buschow, *Phys. Rev. Lett.* **50**, 2024 (1983).
- [2] V. Yu. Irkhin and M. I. Katsnelson, *Uspekhi Fiz. Nauk* **164**, 705 (1994) [*Phys. Usp.* **37**, 659 (1994)].
- [3] W. E. Pickett and J. Moodera, *Phys. Today* **54** (5), 39 (2001).
- [4] G. A. Prinz, *Science* **282**, 1660 (1998).
- [5] A. Biswas and A.K. Raychaudhuri, *J. Phys.: Condens. Matter* **8**, L739 (1996).
- [6] J. Y. T. Wei, N. C. Yeh, R. P. Vasquez, *Phys. Rev. Lett.* **79**, 5150 (1997).
- [7] J. H. Park, E. Vescovo, H. J. Kim, C. Kwon, R. Ramesh, and T. Venkatesan, *Nature* **392**, 794 (1998).
- [8] B. Nadgorny, I. I. Mazin, M. Osofsky, R. J. Soulen, P. Broussard, R. M. Stroud, D. J. Singh, V. G. Harris, A. Arsenov, and Ya. Mukovskii, *Phys. Rev. B* **63**, 184433 (2001).
- [9] D. M. Edwards and J. A. Hertz, *J. Phys. F* **3**, 2191 (1973).
- [10] V. Yu. Irkhin and M. I. Katsnelson, *Fizika Tverdogo Tela* **25**, 3383 (1983) [Engl. Transl.: *Sov. Phys. - Solid State* **25**, 1947 (1983)]; *J. Phys. C* **18**, 4173 (1985).
- [11] M. I. Auslender and V. Yu. Irkhin, *J. Phys. C* **18**, 3533 (1985).
- [12] V. Yu. Irkhin and M. I. Katsnelson, *J. Phys.: Condens. Matter* **2**, 7151 (1990).
- [13] M. I. Auslender and V. Yu. Irkhin, *Sol. State Commun.* **56**, 703 (1985).
- [14] V. Yu. Irkhin and M. I. Katsnelson, *Eur. Phys. J. B* **19**, 401 (2001).
- [15] V. Yu. Irkhin and M. I. Katsnelson, *Eur. Phys. J. B* **43**, 479 (2005).
- [16] G. Tkachov, E. McCann, and V. I. Fal’ko, *Phys. Rev. B* **65**, 024519 (2001).
- [17] V. Yu. Irkhin and M. I. Katsnelson, *Eur. Phys. J. B* **30**, 481 (2002).
- [18] E. McCann and V. I. Fal’ko, *Phys. Rev. B* **68**, 172404 (2003).
- [19] L. Chioncel, M. I. Katsnelson, R. A. de Groot, and A. I. Lichtenstein, *Phys. Rev. B* **68**, 144425 (2003).
- [20] L. Chioncel, M. I. Katsnelson, G. A. de Wijs, R. A. de Groot, and A. I. Lichtenstein, *Phys. Rev. B* **71**, 085111 (2005).
- [21] P. Nozieres, *Theory of Interacting Fermi Systems* (Benjamin, New York, 1964); D. Pines and P. Nozieres, *The Theory of Quantum Liquids* (Benjamin, New York, 1966).
- [22] S. V. Vonsovsky and M. I. Katsnelson, *Quantum Solid State Physics* (Springer, Berlin, 1989).
- [23] V. Yu. Irkhin, M. I. Katsnelson, and A. V. Trefilov, *Physica C* **160**, 397 (1989); *Zh. Eksp. Theor. Fiz.* **105**, 1733 (1994) [*Sov. Phys. JETP* **78**, 936 (1994)].
- [24] R. Wiesendanger, H.-J. Guentherodt, G. Guentherodt, R.J. Cambino, and R. Ruf, *Phys. Rev. Lett.* **65**, 247 (1990); S. Heinze, M. Bode, A. Kubetzka, O. Pietzsch, X. Nie, S. Blügel, and R. Wiesendanger, *Science* **288**, 1805 (2000); M. Kleiber, M. Bode, R. Ravlić, and R. Wiesendanger, *Phys. Rev. Lett.* **85**, 4606 (2000).
- [25] G. D. Mahan, *Many-Particle Physics* (Plenum Press, New York, 1990), Sect. 9.3.
- [26] J. Tersoff and D. R. Hamann, *Phys. Rev. B* **31**, 805 (1985).
- [27] V.A. Ukraintsev, *Phys. Rev. B* **53**, 11176 (1996).

- [28] M. I. Katsnelson and D. M. Edwards, J. Phys.: Condens. Matter **4**, 3289 (1992).
- [29] V. Yu. Irkhin and M. I. Katsnelson, Fiz. Tverd. Tela **26**, 3055 (1984).
- [30] V. Yu. Irkhin and M. I. Katsnelson, Phys. Rev. B **72**, 054421 (2005).
- [31] K.-I. Kobayashi, T. Kimura, H. Sawada, K. Terakura, and Y. Tokura, Nature **395**, 677 (1998).
- [32] M. I. Auslender, M. I. Katsnelson, and V. Yu. Irkhin, Physica B **119**, 309 (1983).
- [33] V. Yu. Irkhin and A. V. Zarubin, Phys. Rev. B **70**, 035116 (2004).
- [34] D. M. Edwards, J. Phys. C **16**, L327 (1983).
- [35] M. I. Auslender and V. Yu. Irkhin, Sol. State Commun. **50**, 1003 (1984).
- [36] E. Kisker, G. Baum, A. Mahan, W. Raith and B. Reihl, Phys.Rev. B**18**, 2256 (1978).
- [37] M. J. Otto, R. A. M. van Woerden, P. J. van der Valk, J. Wijngaard, C. F. van Bruggen, and C. Haas, J. Phys.: Cond. Mat.**1**, 2351 (1989).
- [38] R. Skomski and P. A. Dowben, Europhys. Lett. **58**, 544 (2002).
- [39] G. A. de Wijs and R. A. de Groot, Phys. Rev. B **64**, 020402 (2001).
- [40] O. Újsághy, J. Kroha, L. Szunyogh, and A. Zawadowski, Phys. Rev. Lett. **85**, 2557 (2000).
- [41] V. Madhavan, W. Chen, T. Jamneala, and M. F. Crommie, Phys. Rev. B **64**, 165412 (2001).
- [42] O. Yu. Kolesnychenko, G. M. M. Heijnen, A. K. Zhuravlev, R. de Kort, M. I. Katsnelson, A. I. Lichtenstein, and H. van Kempen, Phys. Rev. B **72**, 085456 (2005).
- [43] S.-J. Tang, Ismail, P. T. Sprunger, and E. W. Plummer, Phys. Rev. B **65**, 235428 (2002).
- [44] E.W. Plummer, Junren Shi, S.-J. Tang, Eli Rotenberg, S.D. Kevan, Prog. Surf. Sci. **74**, 251 (2003).
- [45] Junren Shi, S.-J. Tang, Biao Wu, P. T. Sprunger, W. L. Yang, V. Brouet, X. J. Zhou, Z. Hussain, Z.-X. Shen, Zhenyu Zhang, and E.W. Plummer, Phys. Rev. Lett. **92**, 186401 (2004).
- [46] M. I. Katsnelson and A. V. Trefilov, Phys. Rev. B **61**, 1643 (2000).

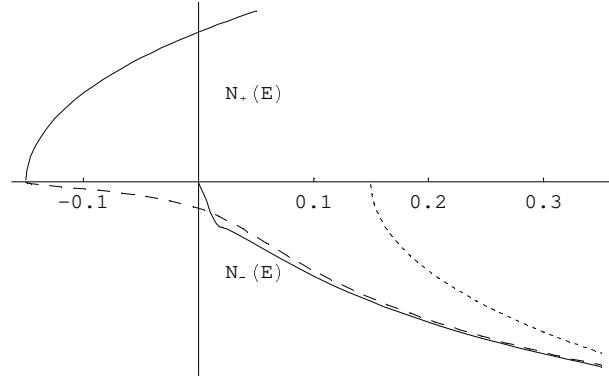


FIG. 1: Density of states in the $s-d$ exchange model of a half-metallic ferromagnet with $S = 1/2, I = 0.3$ for the semielliptic bare band with the width of $W = 2$. The Fermi energy calculated from the band bottom is 0.15 (the energy is referred to E_F). The magnon band is also assumed semielliptic with the width of $\omega_{\max} = 0.02$. The non-quasiparticle tail of the spin-down subband (lower half of the figure) occurs above the Fermi level. The corresponding picture for the empty conduction band is shown by dashed line; the short-dashed line corresponds to the mean-field approximation.

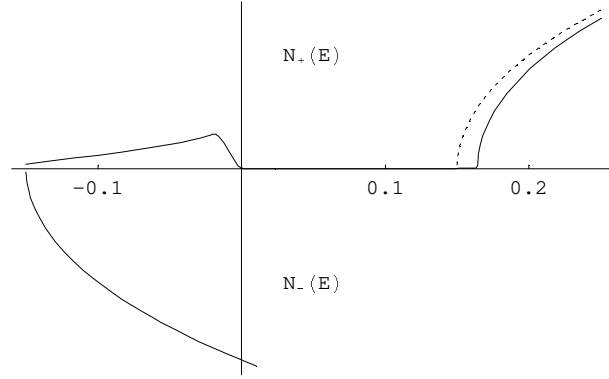


FIG. 2: Density of states in a half-metallic ferromagnet with $I = -0.3 < 0$, other parameters being the same as in Fig.1. The spin-down subband (lower half of the figure) nearly coincides with the bare band shifted by IS . Non-quasiparticle states in the spin-up subbands (upper half of the figure) occur below the Fermi level; the short-dashed line corresponds to the mean-field approximation.

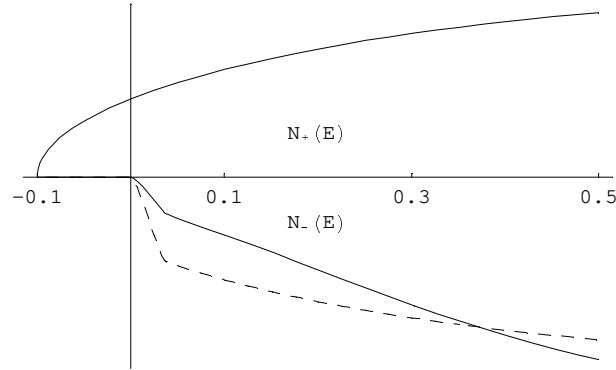


FIG. 3: Density of states in a half-metallic ferromagnet in the $s-d$ model with $I \rightarrow +\infty, S = 1/2$. The Fermi energy calculated from the bare band bottom is 0.1 (concentration of conduction electrons is $c = 0.019$). The dashed line shows the function $-(1/\pi)\text{Im}\bar{R}(E)$.

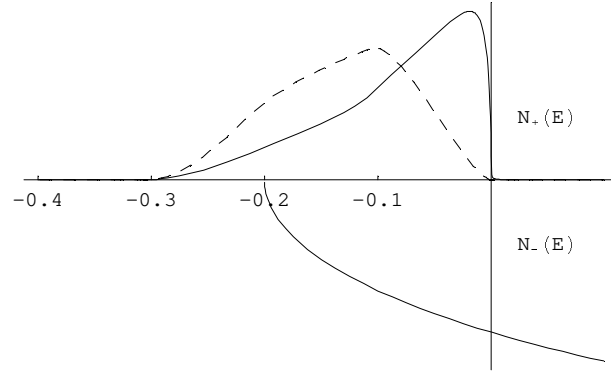


FIG. 4: Density of states in a half-metallic ferromagnet in the s-d model with $I \rightarrow -\infty, S = 1/2$. The Fermi energy calculated from the bare band bottom is 0.2 ($c = 0.034$). The dashed line shows the function $-(1/\pi)\text{Im}\overline{R}^*(E)$.

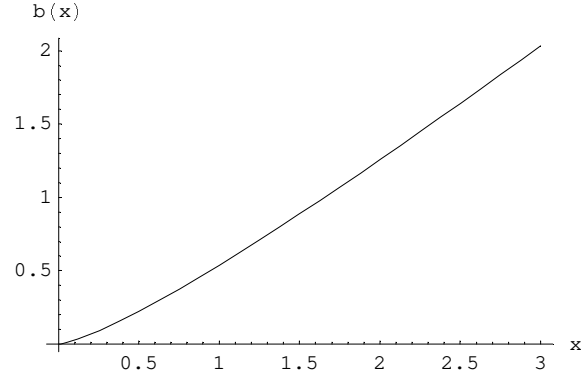


FIG. 5: Plot of the function $b(x)$.

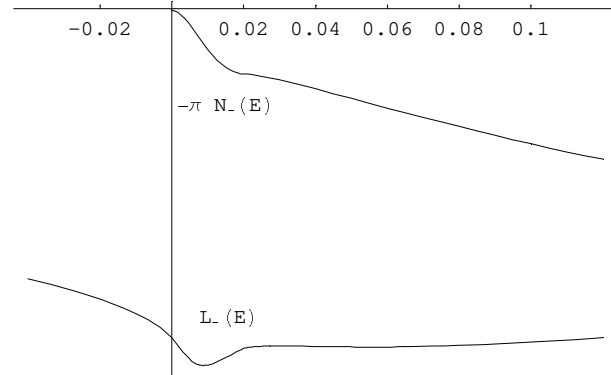


FIG. 6: Plot of the imaginary (upper line) and real (lower line) parts of the Green's function near the Fermi level in a half-metallic ferromagnet with the same parameters as in Fig.1.